Effects of inorganic MnO_2 and ZnO nanofillers on the structural investigations and dielectric behaviour of PVA polymeric materials

B. M. Alotaibi[a,*], H. A. Al-Yousef[a], A. Atta[b,*], F. A.Taher[c,d]
[a]*Physics Department, College of Science, Princess Nourah bint Abdulrahman University, Riyadh, Saudi Arabia*
[b]*Physics Department, College of Science, Jouf University, P.O. Box: 2014, Sakaka, Saudi Arabia*
[c]*Chemistry Department, Faculty of Science, Al-Azhar University (Girls), Nasr city, Cairo, Egypt*
[d]*Al-Azhar Technology Incubator (ATI), Nasr city, Cairo, Egypt*

Different contents of manganese oxide (MnO_2) and zinc oxide (ZnO) were combined with polyvinyl alcohol (PVA) to form flexi MnO_2/PVA as well as ZnO/PVA nanocomposite films. XRD as well SEM methodologies are used to evaluate the properties of the fabricated films. The XRD analysis demonstrates that MnO_2/PVA as well as ZnO/PVA composites were effectively fabricated. The SEM pictures show that MnO_2 and ZnO are uniformly dispersed throughout the PVA polymeric chains. Furthermore, the electrical conductivities, dielectric permittivity, electric moduli behaviors, as well as dielectric impedances of PVA, MnO_2/PVA, ZnO/PVA films were recorded using LCR method in frequencies 10^2 to 10^6 Hz. At 10^5 Hz, the dielectric enhanced from 2.05 for PVA to 5.5 on PVA/5%ZnO and 4.15 for PVA/10%MnO_2, while the conductivities increase from $1.05x10^{-7}$ S/cm for PVA to $4.01x10^{-7}$ S/cm for PVA/5%ZnO and to $5.4x10^{-7}$ S/cm for PVA/10%MnO_2. The current work pave the way to using of ZnO/PVA and MnO_2/PVA flexi nanocomposite films in a different uses including battery, super-capacitors, as well as storage devices.

(Received December 14, 2022; Accepted March 8, 2023)

Keywords: MnO_2/PVA composite, ZnO nanoparticles, Dielectric characteristics, Energy applications

1. Introduction

Ongoing progress is being made toward the manufacture of more flexible dielectric nanocomposites, which can lead to distinctive designated technologies [1]. The nanocomposites films were created by dispersing nano-sized inorganic additives in an organic polymeric matrix [2]. Those composites have been employed in a variety of implementations, such supercapacitors as well as stretchy electrodes [3]. Composite films with distinct structural as well as dielectric properties are used as substances for electrical energy storage instruments [4]. The composite films are important because they merge the polymer's machinability, longevity, as well as ductile qualities with the thermal stability as well as electric conductivities of the nano-additive [5]. As a consequence, by selecting a polymer structure as well as a nanofiller structure, the physical characteristics of the composite material may be altered for intended device uses [6].

Metallic oxide nanoparticles have potential uses in sensing, electrical device development, as well as biomedical activities. Scientists have expressed a desire to select materials that are acceptable for the intended purposes [7]. Because of its good biocompatibility, manganese dioxide (MnO_2) has sparked the attention of nanotechnology research groups [8]. MnO_2 was used as an electro-catalyst for oxygen production as well as reductions in both aqueous and organic electrolyte [9]. MnO_2 is a high-performance substance with exceptional physical and chemical features [10].

* Corresponding authors: aamahmad@ju.edu.sa
https://doi.org/10.15251/JOR.2023.192.175

On the other side, the insertion of inorganic ZnONPs additive into the polymeric chains induces both chemical and structural alterations in the composite samples. ZnONPs is much functional than micron-sized ZnO that enhances the mechanical as well as dielectric qualities of the polymeric chains [11]. ZnO provides greater resistance to deterioration with dispersed uniformity [12]. Several studies have been conducted to investigate the impact of distributing ZnO into the PVA polymer matrices on the conductance and dielectric characteristics of polymeric films [13,14]. The amount of inorganic filler in the polymeric chains influences both the electron transit and the formation of electric pathways [15].

Moreover, PVA polymeric substances can be easily handled and moulded into sheets utilizing different preparation processes [16]. The suggested PVA polymer has undergone significant research as an excellent host lattice for several kinds of fillers nanostructures [17]. Because of its hydrophilicity, chemical resilience, as well as electrical insulation characteristics, PVA is also widely employed in electronic equipment [18,19]. Moreover, PVA with hydroxyl groups possesses a carbon chain backbone that may be used as a hydrogen - bonded source in the production of filler composite materials [20]. This research aims to enhance the electrical conductivity, dielectric characteristics, as well as energy density ability of MnO_2/PVA and ZnO/PVA flexi composite films to be used in the dielectric devices.

2. Experimental work

The PVA solutions were mixed with ZnO (0.5% and 5%) as well as MnO_2 (2.5% and 10%) utilizing solution cast fabrication methodology [21]. The MnO_2/PVA as well as ZnO/PVA nanocomposites were casted, placed into petri plates, then left to dry in a 40 °C oven for a 24-hour period. Subsequently, the films cut into 1.5×1.5 cm portions for made the characterization. The formed films had mean thicknesses of 0.5 mm. XRD (Shimadzu-6000) was used to record out the structural characteristics of these films. Scanning electron microscopy (SEM; JEOL; Japan) was used to examine the surface changes of MnO_2/PVA and ZnO/PVA films. The dielectric characteristics are measured with a programmed LCR meter (3531Z, Hioki, Japan).

3. Results and discussion

Figure 1 depicts the XRD of PVA, MnO_2/PVA, as well as ZnO/PVA samples. The graph represents just one peak for PVA around $2\theta = 19.7^o$, implying that PVA has a semi-crystalline framework. The creation of MnO_2 is proven by the shifting strengths of PVA diffract peaks with increasing manganese dioxide concentration, as illustrated in Fig.1a. Furthermore, the diffraction peaks at $2\theta = 19.7°$ are moved towards to the reduced 2θ, as well as the diffraction intensity increases when compared to PVA [22].

Moreover, as depicted in Fig.1b [23], the major peaks of ZnO are found at scattered inclinations $2\theta = 31.6, 34.4^o$, as well as 36.2^o, corresponded to reflects (100), (002), and (101) planes. The results demonstrate that the composite films comprise of just 2 phases: PVA as well as ZnO, without any additional phases, supporting the effective preparation of ZnO/PVA composites [24]. The peak intensity of PVA at $2\theta = 19.7^o$ is modified by MnO_2 as well as ZnO, as illustrated in Fig.1a,b respectively, indicating that MnO_2 and/or ZnO are effectively incorporated in the PVA. Further, the enlargement of the full width half maximum (FWHM) of the PVA diffracting peak at 19.7^o reveals substantial MnO_2 and ZnO diffusibility into the PVA polymeric chains. The crystallite MnO_2 and ZnO size are estimated by Debye-Scherrer formula, $D= (0.9*\lambda)/(\beta \cos\theta)$ [24]. The recorded D of MnO_2 is 28.4 nm and 32 nm for ZnO.

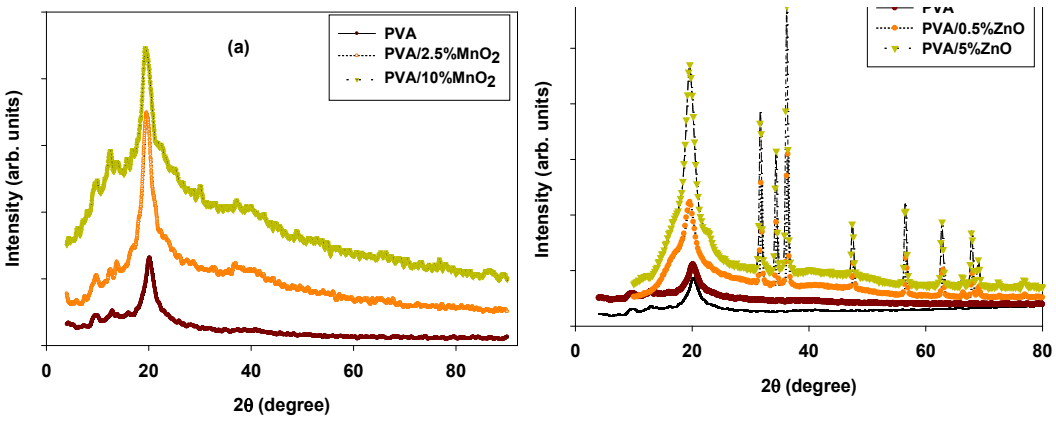

Fig. 1. XRD of (a) PVA, PVA/2.5%MnO_2, PVA/10%MnO_2. (b) PVA, PVA/0.5%ZnO as well as PVA/5%ZnO.

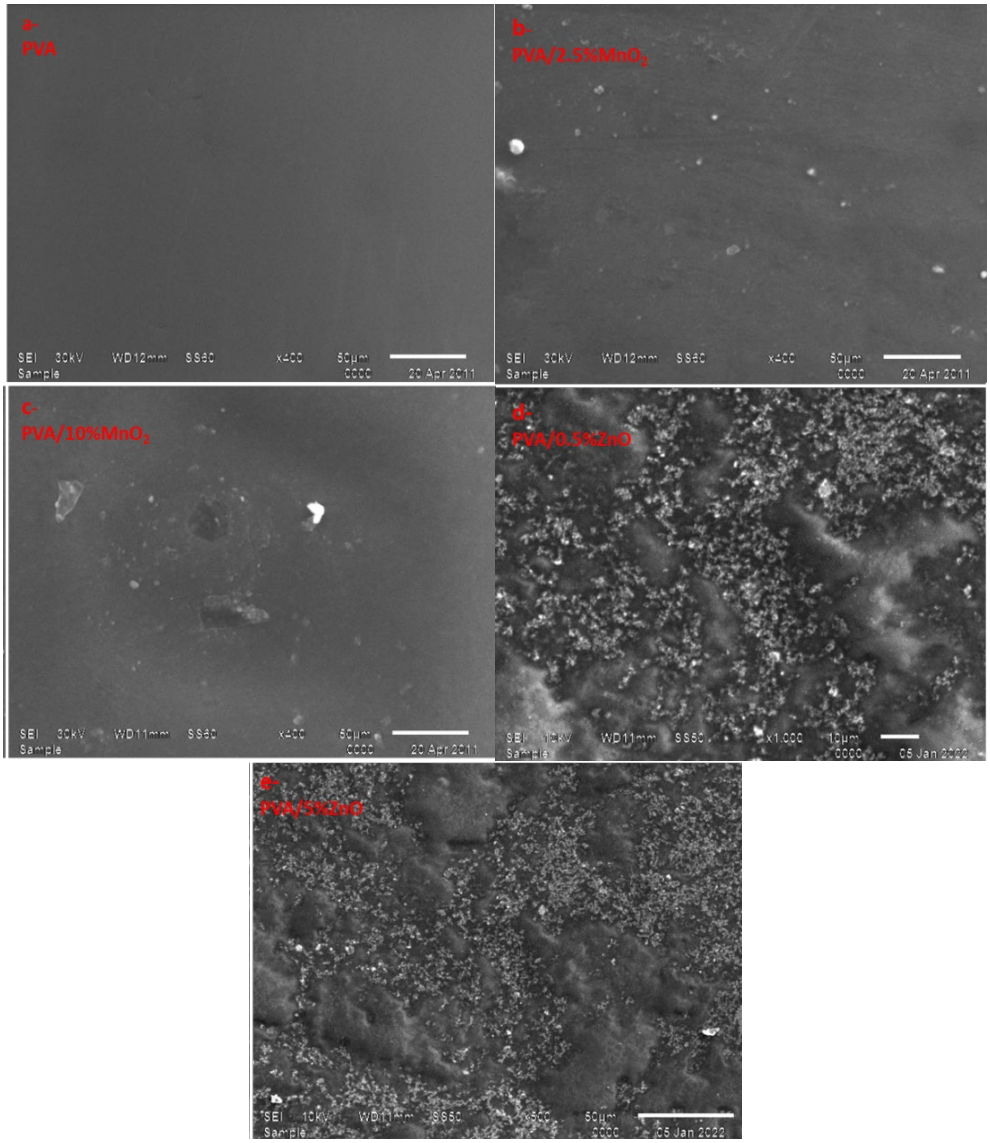

Fig. 2. SEM micrographs of (a) pure PVA, (b) PVA/2.5%MnO_2,(c) PVA/10%MnO_2, (d) PVA/0.5%ZnO and (e) PVA/5%ZnO films.

SEM Micrographs of PVA, PVA/2.5%MnO_2, PVA/10%MnO_2, PVA/0.5%ZnO, as well as PVA/5%ZnO films are shown in Figures 2(a-e). Fig. 2a exhibits the morphological characteristics of the pure PVA film, demonstrating that it is uniform as well as homogeneous [25]. Besides that, the SEM pictures of the PVA film upon incorporation of MnO_2 and ZnO demonstrated the existence of granule shapes as well as the spread of white points. This reveals the presence of MnO_2 and ZnO in the polymer matrices, as displayed in Figs. 2(b-e). The morphologies of the images are showing the integration of MnO_2 and ZnO with effective dispersal in PVA. The homogenous spread of MnO_2 and ZnO in PVA matrix is enhanced by increasing the filler (MnO_2 and ZnO) content as illustrated in Figure 2(b,c) for MnO_2 and as as seen in Fig. 2(d,e) for ZnO. This demonstrated that MnO_2 as well as ZnO generated alterations in PVA nanostructures due to their excellent interactions with PVA [26].

The constant $\boldsymbol{\varepsilon}$`, that means a material's ability to store electrical charges, is derived using capacitance measurements by [27].

$$\varepsilon` = \frac{C \,.\, d}{\varepsilon_o \,.A} \tag{1}$$

C is capacitance, *A* denoted to electrode area, $\boldsymbol{\varepsilon_o}$ is permittivity ~8.85x10^{-12} F/m, and *d* is thickness. Figure 3 depicts the $\boldsymbol{\varepsilon}$` as a frequency dependent variation for PVA, PVA/0.5%ZnO, PVA/5%ZnO, PVA/2.5%MnO_2, as well as PVA/10%MnO_2. The dielectric constant is altered by the operating frequency as a result of the free charge carriers that move over the substance. And raising the implemented frequency results in an alteration in $\boldsymbol{\varepsilon}$`, since the space charge contributions is critical in the polarizability processes [28]. At frequency $10^5$ Hz, the $\boldsymbol{\varepsilon}$` rises from 2.05 for pure PVA to 4.15 for PVA/10%MnO_2 as well as 5.5 for PVA/5%ZnO, as shown in Table 1.

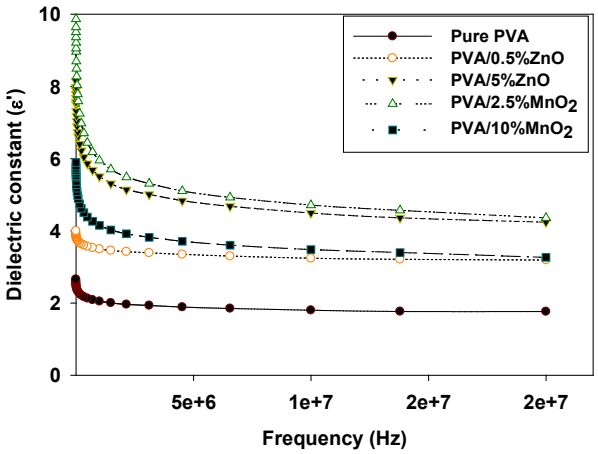

Fig. 3: $\boldsymbol{\varepsilon}$` against frequency of PVA, PVA/0.5%ZnO, PVA/5%ZnO PVA/2.5%MnO_2 as well as PVA/10%MnO_2 samples.

The imaginary dielectric loss $\boldsymbol{\varepsilon}$``, is generally estimated by the using **tanδ** by[29].

$$\varepsilon'' = \varepsilon' \tan\delta \tag{2}$$

Figure 4 depicts the dependence dielectric loss $\boldsymbol{\varepsilon}$`` on frequency for PVA and varied amounts of ZnO as well as $MnO_2$. The $\boldsymbol{\varepsilon}$`` of all films changes as the input frequency rises [30]. The variation in $\boldsymbol{\varepsilon}$`` with frequency is attributable to charging influences that produce a change in electrical oscillations [31]. Table 1 shows that at $10^5$ Hz, the $\boldsymbol{\varepsilon}$`` increases from 0.133 for pristine PVA to 0.72 for PVA/5%ZnO as well as 0.97 for PVA/10%MnO_2. The increase in $\boldsymbol{\varepsilon}$`` is a result of

the enhancement of linkage among PVA with ZnO and MnO_2. The variation in dielectric permittivity's is related to a modification in dipole number that corresponds to polarization as well as dipole structuring [32]. Furthermore, the increased dielectric permittivity's caused by ZnO and MnO_2 are due to the dipolar relaxing characteristic [33]. The dispersal of ZnO and MnO_2 in the PVA polymeric matrix caused alterations in relaxation properties of PVA.

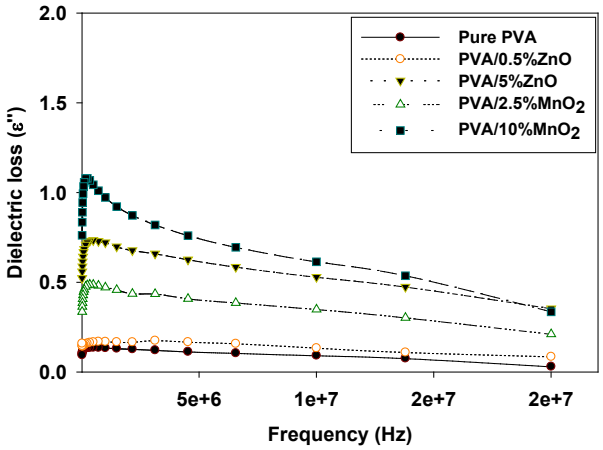

Fig. 4. $\boldsymbol{\varepsilon}$`` *against applied frequency of PVA, PVA/0.5%ZnO, PVA/5%ZnO PVA/2.5%*MnO_2 *and PVA/10%*MnO_2 *samples.*

The modulus ***M*** that is represented by the formula [34]

$$M = \frac{1}{\varepsilon' + i\varepsilon''} = M' + i\,M'' \tag{3}$$

$\mathbf{M}''$ and $\mathbf{M}'$ were the imaginary as well as real components of the electrical moduli, correspondingly, and the real term is $\mathbf{M}' = \frac{\boldsymbol{\varepsilon}'}{\boldsymbol{\varepsilon}'^2 + \boldsymbol{\varepsilon}''^2}$, whereas the imaginary term is $\mathbf{M}'' = \frac{\boldsymbol{\varepsilon}''}{\boldsymbol{\varepsilon}'^2 + \boldsymbol{\varepsilon}''^2}$. Figure 5 depicts the fluctuation of M' with operating frequency for pure PVA, PVA/0.5%ZnO, PVA/5%ZnO, PVA/2.5%MnO_2, and PVA/10%MnO_2 films.

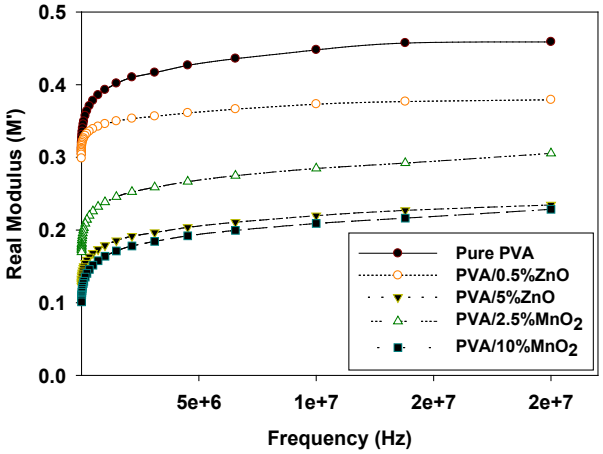

Fig. 5. M' against supplied frequency for PVA, PVA/0.5%ZnO, PVA/5%ZnO, PVA/2.5%MnO_2 *as well as PVA/10%*MnO_2 *films.*

According to the graph, the quantity of $\mathbf{M}'$ varies with the operating frequency of all films that support the polarization electrode and provide a negligible contribution to the substances. Furthermore, the quantities of $\mathbf{M}'$ for the films drop as ZnO and MnO_2 concentrations increase due to segmented chain movement as well as free carriers [35]. The $\mathbf{M}'$ coefficients in PVA steadily decrease as the ZnO and MnO_2 increase. Table 1 shows that at 10^5 Hz, the $\mathbf{M}'$ decreases from 0.393 for pure PVA to 0.164 for PVA/10%MnO_2 as well as 0.178 for PVA/5%ZnO. This is because ZnO and MnO_2 rise with conductivity thus diminish composites film relaxations.

M" with operating frequency for PVA, PVA/0.5%ZnO, PVA/5%ZnO, PVA/2.5%MnO_2, as well as PVA/10%MnO_2 films is represented in Fig.6. The M" changes due to the orientated their-self at low frequencies, allowing for higher permittivity [36]. At 10^5 Hz, the modulus M" is reduced from $3.63*10^{-2}$ for pure PVA to $2.33*10^{-2}$ for PVA/5%ZnO as well as $2.67*10^{-2}$ for PVA/10%MnO_2, as shown in Table 1. The reductions in electrical modulus value are due to the involvement of free carriers [37]. As a result, the charge carriers increases, the conductivity increases, and hence electrical permittivity reduced.

The relaxation time $\boldsymbol{\tau_r}$ of the is estimated by raising concentrations of ZnO or MnO_2, by [38].

$$\tau_r = \frac{1}{2\pi f_p} \tag{4}$$

The fluctuation in $\boldsymbol{\tau_r}$ values is due to the interaction of ZnO and MnO_2 with PVA, whereas $\boldsymbol{f_p}$ is the applicable frequency rating based to the relaxation peaks. The anticipated relaxation time drops from $7.4*10^{-8}$ sec for pristine PVA to $5.1*10^{-8}$ sec for PVA/0.5%ZnO, to $3.5*10^{-8}$ sec for PVA/5%ZnO, and reduced to $4.9*10^{-8}$ sec for PVA/2.5%MnO_2 and to $3.3*10^{-8}$ sec for PVA/10%MnO_2. This is due to the fact that ZnO and MnO_2 reduce the time necessary for dipole orienting. This finding validates the flexibility and effective dispersal of ZnO and MnO_2 within PVA [39]. The decrease in relaxation time τ_r caused by ZnO and MnO_2 is owing to their mobility and high conductivity.

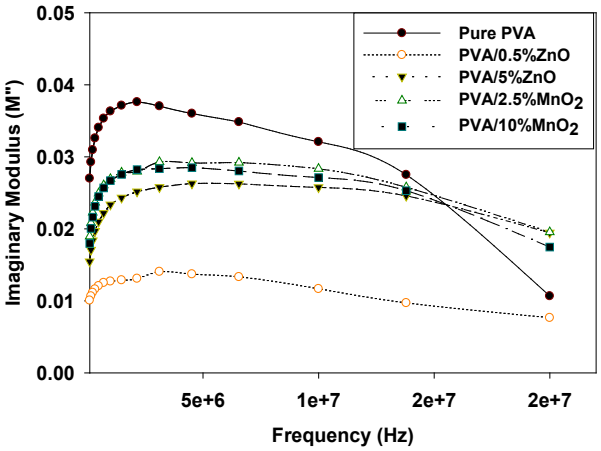

Fig. 6. M" against frequency for PVA, PVA/0.5%ZnO, PVA/5%ZnO PVA/2.5%MnO_2 as well as PVA/10%MnO_2 samples.

Moreover, the following method [40] is used to calculate impedance Z*.

$$Z^* = Z' + iZ'' \tag{5}$$

Z* is impedance, Z′ is real impedance, and Z′′ is imaginary impedance. Z′ reduced by frequency as seen in Fig.7. Conduction rises as the number of free charges grows while the impedance remains constant [41]. The films that have been treated with ZnO and MnO_2 act comparable to PVA films. As previously stated, the induced charge free carriers reduce the Z' drop by increasing ZnO and MnO_2. Furthermore, when ZnO and MnO_2 concentrations grew, conductivity as well as free carriers rose, altering the impedance.

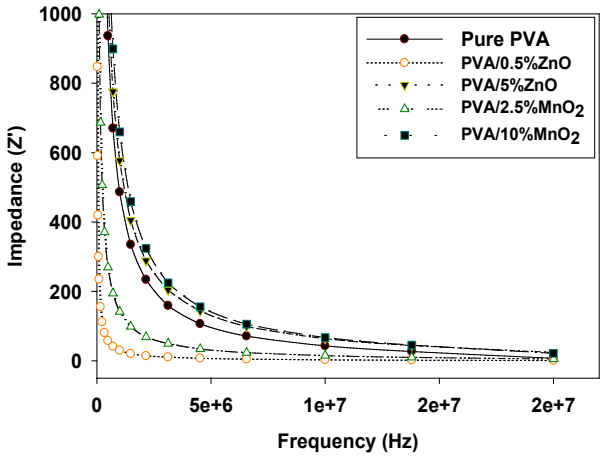

Fig. 7. Z' against frequency for PVA, PVA/0.5%ZnO, PVA/5%ZnO PVA/2.5%MnO_2 as well as PVA/10%MnO_2 samples.

Energy density (U), that measure the ability to store energy, is given by [42]:

$$U = \frac{1}{2}\,\varepsilon'\varepsilon_O\,E^2 \tag{6}$$

E corresponds electric field, as E = 1 V/mm, ε' is the dielectric constant and ε_O= 8.85*10^{-12} F/m. The energy density U is plotted against frequencies for PVA, PVA/0.5%ZnO, PVA/5%ZnO, PVA/2.5%MnO_2, as well as PVA/10%MnO_2 films, as illustrated in Fig. 8. As demonstrated in Fig.8, there is a significant improvement in the energy density of PVA/MnO_2 and PVA/ZnO composite films when compared to untreated PVA. As shown in Table 1, the energy density of PVA at 10^5 Hz is 0.91*10^{-5} J/m^3, increasing to 1.83*10^{-5} J/m^3 for PVA/10%MnO_2 and 2.43*10^{-5} J/m^3 for PVA/5%ZnO. This is due to the inclusion of ZnO and MnO_2 within PVA resulting in faster charge transfer within PVA. These findings support the effective inclusion of ZnO and MnO_2 into the PVA polymeric chains, which increased the dielectric response and thus energy storage capabilities.

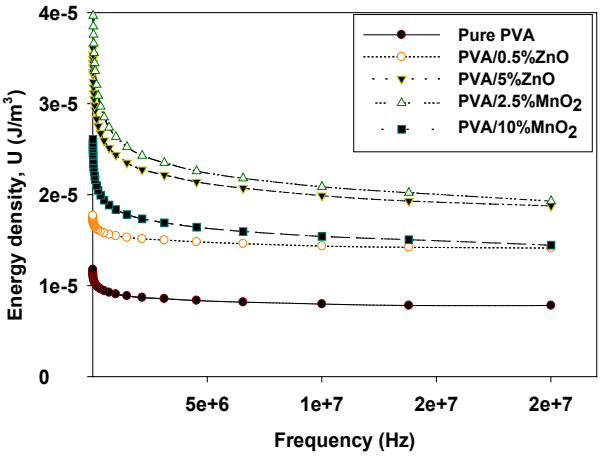

Fig. 8. U variation with frequency of PVA, PVA/0.5%ZnO, PVA/5%ZnO PVA/2.5%MnO_2 and PVA/10%MnO_2 samples.

Table 1. $\varepsilon`$, $\varepsilon``$, M', M'' , Z', σ_{ac} and U for PVA, PVA/0.5%ZnO, PVA/5%ZnO PVA/2.5%MnO_2 and PVA/10%MnO_2 samples.

	$\varepsilon`$	$\varepsilon``$	M'	M''	σ_{ac} (S/cm)	$U(J/m^3)$
Pristine PVA	2.05	0.133	0.393	0.0363	$1.05*10^{-7}$	$0.91*10^{-5}$
PVA/0.5%ZnO	3.49	0.167	0.345	0.0127	$0.71*10^{-7}$	$1.54*10^{-5}$
PVA/5%ZnO	5.50	0.720	0.178	0.0233	$4.01*10^{-7}$	$2.43*10^{-5}$
PVA/2.5%MnO_2	5.95	0.469	0.238	0.0269	$2.6*10^{-7}$	$2.63*10^{-5}$
PVA/10%MnO_2	4.15	0.970	0.164	0.0267	$5.4*10^{-7}$	$1.83*10^{-5}$

The relationship between electrical conductivity σ_{ac} with frequency exponent (S) is represented by the equation [43]:

$$\sigma_{ac} = A\omega^{S} \tag{7}$$

$\boldsymbol{\omega}$ is frequency, S is frequency exponent, that is usually below than or equals to one. Fig.9 depicts the electric conductivities $\boldsymbol{\sigma_{ac}}$ with frequency of PVA, PVA/0.5%ZnO, PVA/5%ZnO, PVA/2.5%MnO_2, and PVA/10%MnO_2 films. Interestingly, the ac electrical conductivity of all films increases with higher frequency, possibly attributed to the increase in mobility of charge carriers with applicable electric fields [44]. At the operating frequency of 1MHz, the $\boldsymbol{\sigma_{ac}}$ is raised from $1.05*10^{-7}$ S/cm for pristine PVA to $4.01*10^{-7}$ S/cm for PVA/5%ZnO and to $5.4*10^{-7}$ S/cm for PVA/10%MnO_2 as shown in Table 1. The inclusion of ZnO and MnO_2 within PVA will lowering the potential barrier of PVA [45,46].

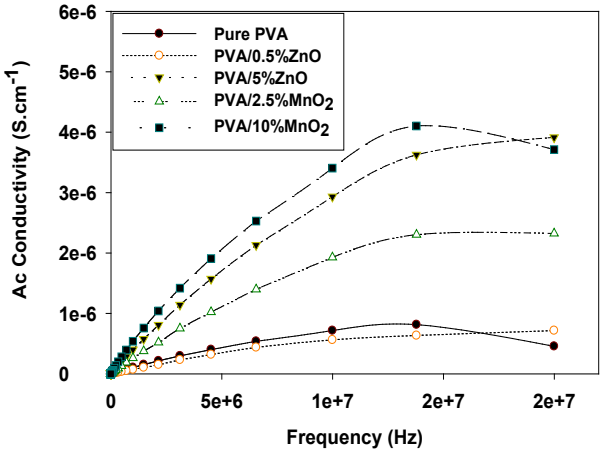

Fig. 9. Ac conductivities (σ_{ac}) against frequency for PVA, PVA/0.5%ZnO, PVA/5%ZnO PVA/2.5%MnO_2 as well as PVA/10%MnO_2 samples.

The calculated S from Figure 10 is changed from 0.995 for pure PVA to 0.985 for PVA/0.5%ZnO to 0.972 for PVA/5%ZnO. And it is changed to 0.980 for PVA/2.5%MnO_2 and to 0.930 for PVA/10%MnO_2. This variation in S values is caused by variations in defect density with ZnO and MnO_2. The given relationship [47] is utilized to compute the potential barrier height W_M.

$$W_m = \frac{6K_BT}{1-S} \tag{8}$$

k_B is Boltzmann constant, T is temperature, S is frequency exponent, and W_m is the energy needed to transport electrons from one place to infinity. As illustrated in Fig.10, the computed potential barrier W_m changed with rising ZnO content, from 31.3 eV for pristine PVA to 10.4 eV for PVA/0.5%ZnO, 6.2 for PVA/5%ZnO, 7.83 for PVA /2.5%MnO_2, and 2.24 eV for PVA/10%MnO_2. This variation in potential barrier W_m is due to the enhancement of crystalline structure with the additions of inorganic ZnO and MnO_2 nanofilles.

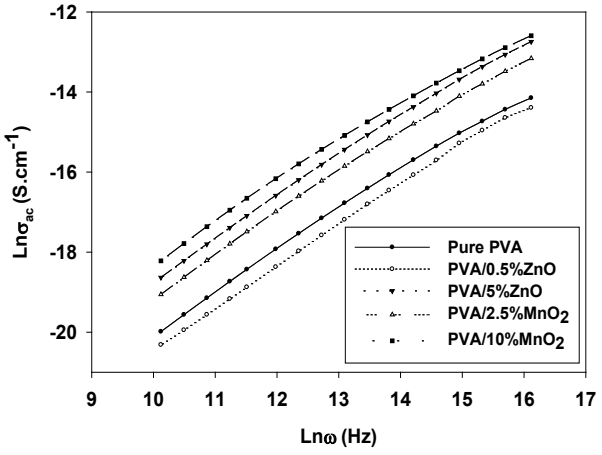

Fig. 10. Ln (σ_{ac}) against Ln (ω) for PVA, PVA/0.5%ZnO, PVA/5%ZnO PVA/2.5%MnO_2 and PVA/10%MnO_2 samples.

4. Conclusion

MnO_2/PVA and ZnO/PVA nanocomposite films were successfully synthesized as evidenced by XRD as well as SEM data. The analysis showed that MnO_2 and ZnO react well with the PVA network. Furthermore, electrical conductivity and dielectric factors such as dielectric constants, dielectric losses, as well as electrical energy densities are examined. At 10^5 Hz, the dielectric constant ε' rises from 2.05 for pure PVA to 4.15 for PVA/10%MnO_2 and to 5.5 for PVA/5%ZnO at frequency 10^5 Hz. Moreover, PVA has energy density of $0.91*10^{-5}$ J/m^3, enhanced to $1.83*10^{-5}$ J/m^3 for PVA/10%MnO_2, and to $2.43*10^{-5}$ J/m^3 for PVA/5%ZnO. Furthermore, the relaxation time is lowered from 7.4×10^{-8} sec for PVA to 3.5×10^{-8} sec for PVA/5%ZnO and 3.3×10^{-8} sec for PVA/10%MnO_2. This is due to the fact that ZnO and MnO_2 reduce the period necessary for dipole orienting. The electrical data revealed that the inclusion of MnO_2 and ZnO are enhanced the dielectric characteristics of the PVA. Besides, electric modulus behaviors are confirming that films have significantly superior impedance as well as dielectric characteristics than pure PVA. Moreover, the increased in energy density efficiencies of PVA films with MnO_2 and ZnO would pave the way for the use of flexi MnO_2/PVA and ZnO/PVA films in a variety of prospective systems for energy storing as well as super-capacitor.

Acknowledgments

The authors extend their appreciation to the Deputyship for Research & Innovation, Ministry of Education in Saudi Arabia for funding this research work through the project number RI-44-0045

References

[1] Zwawi, M., Attar, A., Al-Hossainy, A. F., Abdel-Aziz, M. H., Zoromba, M. S. (2021), Chemical Papers, 75(12), 6575-6589; https://doi.org/10.1007/s11696-021-01830-5

[2] Chaturvedi, A. K., Pappu, A., Srivastava, A. K., & Gupta, M. K. (2021), Materials Letters, 301, 130323; https://doi.org/10.1016/j.matlet.2021.130323

[3] Abutalib, M. M., & Rajeh, A. (2020), Polymer Testing, 91, 106803; https://doi.org/10.1016/j.polymertesting.2020.106803

[4] Li, D., Liu, Y., Shi, S., Li, Y., Geng, C., Xu, S. (2021), Journal of Materials Chemistry C, 9(8), 2873-2881; https://doi.org/10.1039/D0TC05425A

[5] Chaudhuri, B., Ghosh, S., Mondal, B., & Bhadra, D. (2022), Materials Science and Engineering: B, 275, 115500; https://doi.org/10.1016/j.mseb.2021.115500

[6] Altunkaynak, F., Okur, M., & Saracoglu, N. (2022), Journal of Drug Delivery Science and Technology, 68, 103099; https://doi.org/10.1016/j.jddst.2022.103099

[7] Prakash, T., Kumar, E. R., Neri, G., Bawazeer, T. M., Alkhamis, K., Munshi, A., ... & El-Metwaly, N. M. (2022), Ceramics International, 48(1), 1223-1229; https://doi.org/10.1016/j.ceramint.2021.09.207

[8] Dawadi, S., Gupta, A., Khatri, M., Budhathoki, B., Lamichhane, G., & Parajuli, N. (2020), Bulletin of Materials 43(1), 1-10; https://doi.org/10.1007/s12034-020-02247-8

[9] Hill, L. I., Portal, R., Verbaere, A., & Guyomard, D. (2001), Electrochemical and Solid-State Letters, 4(11), A180; https://doi.org/10.1149/1.1402495

[10] Wang, W., Kan, Y., Yu, B., Pan, Y., Liew, K. M., Song, L., & Hu, Y. (2017), Composites Part A: Applied Science and Manufacturing, 95, 173-182; https://doi.org/10.1016/j.compositesa.2017.01.009

[11] Zargar, R. A. (2022), Scientific Reports, 12(1), 1-10; https://doi.org/10.1038/s41598-022-13767-0

[12] Liu, X., Wang, G., Zhi, H., Dong, J., Hao, J., Zhang, X., ... & Liu, B. (2022), Coatings, 12(5), 695; https://doi.org/10.3390/coatings12050695

[13] Liu, H., Liu, W., Hu, D., Ma, W., & Deng, B. (2022), Colloids and Surfaces A: Physicochemical and Engineering Aspects, 129311; https://doi.org/10.1016/j.colsurfa.2022.129311

[14] Hui, Z., Haonan, Z., Hao, R., & Huamin, Z. (2022), International Journal of Biological Macromolecules, 209, 1465-1476; https://doi.org/10.1016/j.ijbiomac.2022.04.127

[15] Mohammed, M. I., Khafagy, R. M., Hussien, M. S., Sakr, G. B., Ibrahim, M. A., Yahia, I. S., & Zahran, H. Y. (2022), Journal of Materials Science: Materials in Electronics, 33(4), 1977-2002; https://doi.org/10.1007/s10854-021-07402-3

[16] Abdelhamied, M. M., Abdelreheem, A. M., & Atta, A. (2022), Plastics, Rubber and Composites, 51(1), 1-12; https://doi.org/10.1080/14658011.2021.1928998

[17] Mohammed, M. I., Yahia, I. S., & El-Mongy, S. A. (2022), Optical and Quantum Electronics, 54(9), 1-23; https://doi.org/10.1007/s11082-022-03981-5

[18] Atta, A., Abdelhamied, M. M., Abdelreheem, A. M., & Althubiti, N. A. (2022); Inorganic Chemistry Communications, 135, 109085; https://doi.org/10.1016/j.inoche.2021.109085

[19] Abdelhamied, M. M., Atta, A., Abdelreheem, A. M., Farag, A. T. M., & El Sherbiny, M. A. (2021), Inorganic Chemistry Communications, 133, 108926; https://doi.org/10.1016/j.inoche.2021.108926

[20] Atta, M. R., Alsulami, Q. A., Asnag, G. M., & Rajeh, A. (2021), Journal of Materials Science: Materials in Electronics, 32(8), 10443-10457; https://doi.org/10.1007/s10854-021-05701-3

[21] Atta, A., Abdel Reheem, A. M., & Abdeltwab, E. (2020), Surface Review and Letters, 27(09), 1950214; https://doi.org/10.1142/S0218625X19502147

[22] Pashameah, R. A., El-Sharnouby, M., El-Askary, A., El-Morsy, M. A., Ahmed, H. A., & Menazea, A. A. (2022), Journal of Inorganic and Organometallic Polymers and Materials, 1-10; https://doi.org/10.1007/s10904-022-02311-2

[23] Abdeltwab, E., & Atta, A. (2021), Surface Innovations, 40, 1-9.

[24] El-Dafrawy, S. M., Tarek, M., Samra, S., & Hassan, S. M. (2021), Scientific Reports, 11(1), 1-11; https://doi.org/10.1038/s41598-021-90846-8

[25] Abdeltwab, E., & Atta, A. (2021), International Journal of Modern Physics B, 35(30), 2150310; https://doi.org/10.1142/S0217979221503100

[26] Majeed, A. H., Al-Tikrity, E. T. B., & Hussain, D. H. (2021), Polymers and Polymer Composites, 29(7), 1089-1100; https://doi.org/10.1177/0967391120951406

[27] Ishaq, S., Kanwal, F., Atiq, S., Moussa, M., Azhar, U., Gul, I., & Losic, D. (2018), Results in Physics, 11, 540-548; https://doi.org/10.1016/j.rinp.2018.09.049

[28] Atta, A. (2020), Surface Innovations, 9(1), 17-24; https://doi.org/10.1680/jsuin.20.00020

[29] Atta, A., Lotfy, S., & Abdeltwab, E. (2018), Journal of Applied Polymer Science, 135(33), 46647; https://doi.org/10.1002/app.46647

[30]Singla, M.; Sehrawat, R.; Rana, N.; Singh, K., Journal of Nanoparticle Research 2011, 13 (5), 2109-2116; https://doi.org/10.1007/s11051-010-9968-4

[31] Zhang, Y.; Wang, Y.; Deng, Y.; Li, M.; Bai, J., ACS applied materials & interfaces 2012, 4 (1), 65-68; https://doi.org/10.1021/am2016156

[32] Kumar, M.; Srivastava, N., Journal of Non-Crystalline Solids 2014, 389, 28-34; https://doi.org/10.1016/j.jnoncrysol.2014.02.002

[33]Wang, G.-S.; Wu, Y.-Y.; Zhang, X.-J.; Li, Y.; Guo, L.; Cao, M.-S., Journal of Materials Chemistry A 2014, 2 (23), 8644-8651; https://doi.org/10.1039/C4TA00485J

[34] I. Latif, E.E. AL-Abodi, D.H. Badri, J. Al Khafagi, American Journal of Polymer Science 2 (2012) 135-140; https://doi.org/10.5923/j.ajps.20120206.01

[35] R. Thangarasu, N. Senthilkumar, B. Babu, K. Mohanraj, J. Chandrasekaran, O. Balasundaram, Journal of Advanced Physics 7 (2018) 312-318;

https://doi.org/10.1166/jap.2018.1442
[36] Wu, W., Huang, X., Li, S., Jiang, P., & Toshikatsu, T. (2012), The Journal of Physical Chemistry C, 116(47), 24887-24895; https://doi.org/10.1021/jp3088644
[37] Hemalatha, K. S., Sriprakash, G., Ambika Prasad, M. V. N., Damle, R., & Rukmani, K. (2015), Journal of Applied physics, 118(15), 154103; https://doi.org/10.1063/1.4933286
[38] Choudhary, S. (2017), Physica B: Condensed Matter, 522, 48-56; https://doi.org/10.1016/j.physb.2017.07.066
[39] R. Gupta, R. Kumar, Nano-Structures & Nano-Objects 18 (2019) 100318; https://doi.org/10.1016/j.nanoso.2019.100318
[40] G. Sahu, M. Das, M. Yadav, B.P. Sahoo, J. Tripathy, Polymers 12 (2020) 374; https://doi.org/10.3390/polym12020374
[41] S. Atiq, M. Majeed, A. Ahmad, S.K. Abbas, M. Saleem, S. Riaz, S. Naseem, Ceramics International 43 (2017) 2486-2494; https://doi.org/10.1016/j.ceramint.2016.11.046
[42] W. Jilani, N. Fourati, C. Zerrouki, O. Gallot-Lavallée, H. Guermazi, Journal of Inorganic and Organometallic Polymers and Materials 29 (2019) 456-464; https://doi.org/10.1007/s10904-018-1016-3
[43] Bouaamlat, H., Hadi, N., Belghiti, N., Sadki, H., Naciri Bennani, M., Abdi, F., ... & Abarkan, M. (2020), Advances in Materials Science and Engineering, 2020; https://doi.org/10.1155/2020/8689150
[44] A. Hashim, A. Hadi, Ukrainian Journal of Physics 63 (2018) 754-754; https://doi.org/10.15407/ujpe63.8.754
[45] H. Ahmed, A. Hashim, Egyptian Journal of Chemistry 63 (2020) 805-811.
[46] Prabakaran, S., Nisha, K. D., Harish, S., Archana, J., & Navaneethan, M. (2021), Journal of Alloys and Compounds, 885, 160936; https://doi.org/10.1016/j.jallcom.2021.160936
[47] Abdel Reheem, A.; Atta, A.; Afify, T., Surface Review &Letters 2017, 24 (03),1750038; https://doi.org/10.1142/S0218625X1750038X